

Björn Rabenstein · G. Matthias Ullmann  
Ernst-Walter Knapp

## Calculation of protonation patterns in proteins with structural relaxation and molecular ensembles – application to the photosynthetic reaction center

Received: 30 October 1997 / Revised version: 2 March 1998 / Accepted: 7 March 1998

**Abstract** The conventional method to determine protonation patterns of proteins was extended by explicit consideration of structural relaxation. The inclusion of structural relaxation was achieved by alternating energy minimization with the calculation of protonation pattern in an iterative manner until consistency of minimized structure and protonation pattern was reached. We applied this method to the bacterial photosynthetic reaction center (bRC) of *Rps. viridis* and could show that the relaxation procedure accounts for the nuclear polarization and therefore allows one to lower the dielectric constant for the protein from the typically chosen value of  $\epsilon_p=4$  to a value of  $\epsilon_p=2$  without fundamentally changing the results. Owing to the lower dielectric shielding at  $\epsilon_p=2$ , the charges of the titratable groups interact more strongly, which leads to sampling problems during Monte Carlo titration. We solved this problem by introducing triple moves in addition to the conventional single and double moves. We also present a new method that considers ensembles of protein conformations for the calculation of protonation patterns. Our method was successfully applied to calculate the redox potential differences of the quinones in the bRC using the relaxed structures for the different redox states of the quinones.

**Key words** Bacterial photosynthesis · Electron transfer · Protein electrostatics · Poisson-Boltzmann equation · Conformational flexibility

**Abbreviations** *bRC* Bacterial (photosynthetic) reaction center · *CPU* Central processing unit · *DMF* Dimethylformamide · *MC* Monte Carlo · *MQ* Menaquinone · *Q<sub>A</sub>* Primary quinone · *Q<sub>B</sub>* Secondary quinone · *rms* Root mean square · *UQ* Ubiquinone

B. Rabenstein · G. M. Ullmann · E.-W. Knapp (✉)  
Institut für Kristallographie, Fachbereich Chemie,  
Freie Universität Berlin,  
Takustrasse 6, D-14195 Berlin, Germany  
e-mail: knapp@chemie.fu-berlin.de

### 1 Introduction

Protonation patterns of proteins can be calculated with continuum electrostatic methods. In such an approach, the aqueous solvent is represented by a medium with a high dielectric constant, typically  $\epsilon_s=80$ , and the protein is represented by a cavity with a low dielectric constant. However, the value of the dielectric constant taken for the cavity  $\epsilon_p$  varies considerably, ranging from  $\epsilon_p=1$  (Muegge et al. 1996; Scarsi et al. 1997) to  $\epsilon_p=20$  and larger (Warshel et al. 1984; Antosiewicz et al. 1994; Demchuk and Wade 1996). A high dielectric constant seems to yield better agreement with experimental data, if simplified descriptions of the protein charges are used (Antosiewicz et al. 1994). In those calculations the protonation of a titratable amino acid is modelled by simply placing a unit charge at a central atom of the titratable site. With a more detailed charge model, where several atomic partial charges of the titratable residue are changed upon protonation, good agreement with experimental data was achieved by using a dielectric constant of  $\epsilon_p=4$  (Bashford et al. 1993; Antosiewicz et al. 1996). Apparently, the large value of the dielectric constant ( $\epsilon_p \geq 20$ ) was necessary to compensate for the effects from an unrealistic charge distribution, where a unit charge is placed at a central atom of the titratable site. The dielectric constant of  $\epsilon_p \geq 4$  can be rationalized as follows: A factor of 2 accounts for the effects of electronic polarization, another factor of 2 or more for the effects of nuclear polarization, i. e., for the reorientation of dipoles and displacements of atoms (Warshel and Russel 1984; Warshel and Åqvist 1991; Honig and Nicholls 1995; Warshel et al. 1997).

In this study, we present a method that considers reorientation and relaxation effects explicitly. We do this by an iterative minimization scheme in conjunction with conventional electrostatic calculations. Our goal is to obtain a relaxed molecular structure, where we can use a dielectric constant of  $\epsilon_p=2$  for the protein to obtain similar results as in electrostatic calculations with a dielectric constant of  $\epsilon_p=4$  using an unrelaxed structure. We

also present a new method to calculate protonation patterns that considers an ensemble of protein conformations. Our method differs from other approaches for including multiple conformations in the calculations of titration curves (You and Bashford 1995; Beroza and Case 1996; Buono et al. 1994; Sham et al. 1997; Schaefer et al. 1997; Alexov and Gunner 1997) in several respects. In previous approaches, the conformational changes were done without accounting for intramolecular correlations. Contributions arising from conformational changes of non-titratable residues are not considered or are restricted to conformational changes of hydrogen atoms only (Alexov and Gunner 1997). Furthermore, energy contributions from non-electrostatic interactions (i.e., energy contributions from Lennard-Jones potentials and from bond-length and bond-angle deformation), which cancel as long as only a single conformation is considered, are often neglected. In our method, these effects are all included. Moreover, we do not necessarily run into the combinatorial problem that the number of conformations increases too steeply with the number of titratable groups, since the correlation of conformations from different titratable groups can be considered easily.

We apply our new methods to the bacterial photosynthetic reaction center (bRC) of *Rps. viridis* and compare the results to a recent study without structural relaxation (Rabenstein et al. 1998). The bRC is a pigment-protein complex in the membrane of purple bacteria. It converts light energy into electrochemical energy by coupling photo-induced electron transfer to proton uptake from the cytoplasm. Four polypeptides form the bRC of *Rps. viridis*, the L, H, and M subunits and a tightly bound four-center *c*-type cytochrome. These polypeptides bind fourteen cofactors, one carotenoid, four hemes, four bacteriochlorophylls, two bacteriopheophytins, one non-heme iron, one menaquinone (MQ) and one ubiquinone (UQ). The two quinones are called  $Q_A$  (MQ) and  $Q_B$  (UQ). They play an important role in the coupling between electron and proton transfer by the ability to change their redox state as well as their protonation state during the photosynthetic process. Electronic excitation of the special pair, a bacteriochlorophyll dimer, induces a multi-step electron transfer from the special pair to  $Q_A$ . From there, the electron moves to  $Q_B$ . After this initial reaction, a second electron transfer from  $Q_A$  to  $Q_B$  and two protonation reactions of  $Q_B$  follow, resulting in a dihydroquinone  $Q_BH_2$ . The dihydroquinone leaves its binding site and is replaced by an oxidized UQ from the quinone pool. In our study, we consider the unprotonated quinones only.

We calculate protonation patterns of the bRC with its unprotonated quinones in the different redox states and also the reaction energy of the first and second electron transfer from  $Q_A$  to  $Q_B$ . Similar studies were already done at the bRC of *Rps. viridis* (Lancaster et al. 1996) and of *Rb. sphaeroides* (Beroza et al. 1995). However, these studies did not include conformational variability. Furthermore, the reaction energies of the electron transfer from  $Q_A$  to  $Q_B$  were not calculated (Lancaster et al. 1996) or they were calculated only for the first electron transfer and

did not agree with experimental results (Beroza et al. 1995). In a recent calculation without structural relaxation, we got reaction energies in agreement with experimental results (Rabenstein et al. 1998). This success is probably due to the appropriate quantum-chemically calculated atomic partial charges for the cofactors, which we used. Since conformational changes upon quinone reduction could be observed in experiments (Stowell et al. 1997), it remains interesting to investigate the effects of structural relaxation. In one previous study of the bRC of *Rps. viridis*, an energy minimization scheme was used to obtain relaxed protein conformations (Cometta-Morini et al. 1993). In that work, even the bRC state, where the  $Q_B$  is singly reduced and singly protonated ( $Q_B \cdot H$ ), was considered. However, only a small part of the bRC near  $Q_B$  was included in that computation, and the minimization was performed with the titratable amino acids in their standard protonation state (at pH 7 in solution). Also no reaction energies for electron transfer were calculated.

## 2 Theory

*Calculation of protonation patterns.* The protonation probability  $\langle x_i \rangle$  of a titratable group  $i$  in a protein with  $N$  titratable groups is given by the thermodynamic average (Eq. (1)) over all possible protonation states of this protein (Bashford and Karplus 1991),

$$\langle x_i \rangle = \frac{\sum_{\mathbf{q}} x_i \exp \left[ -\beta \sum_{\mu} x_{\mu} \Delta G_{intr,\mu} + \frac{1}{2} \sum_{v \neq \mu} q_{\mu} q_v W_{\mu v} \right]}{\sum_{\mathbf{q}} \exp \left[ -\beta \sum_{\mu} x_{\mu} \Delta G_{intr,\mu} + \frac{1}{2} \sum_{v \neq \mu} q_{\mu} q_v W_{\mu v} \right]} \quad (1)$$

where  $\beta = (k_B T)^{-1}$ . The value of the  $i$ th component of the  $N$ -component protonation state vector  $\mathbf{q}$  is the total charge of the titratable group  $i$ , which can adopt the values  $-1$  and  $0$  for acids or  $0$  and  $+1$  for bases, in their unprotonated and protonated state respectively;  $x_i$  is unity if the group  $i$  is protonated, and zero if the group  $i$  is unprotonated;  $W_{\mu v}$  is the electrostatic interaction between the titratable groups  $\mu$  and  $v$  if both are in their charged protonation state. The outer sums run over all  $2^N$  possible state vectors  $\mathbf{q}$ . The sums in the exponential functions run over all titratable groups. The energy  $\Delta G_{intr,\mu}$  is required to protonate group  $\mu$  at a given pH-value, while all other titratable groups are in their uncharged protonation state. This energy is related to the so-called intrinsic  $pK_a$ -value of group  $\mu$   $pK_{intr,\mu}$  as given in Eq. (2).

$$\Delta G_{intr,\mu} = - \frac{2,303(pK_{intr,\mu} - pH)}{\beta} \quad (2)$$

We calculated the differences between the intrinsic  $pK_a$ -values  $pK_{intr,\mu}$  in the protein and the  $pK_a$ -values of appropriate model compounds in aqueous solution and the interactions  $W_{\mu v}$  between the titratable group  $\mu$  and  $v$  by a continuum electrostatic method using the program MEAD

(Bashford and Karplus 1990). This program solves the linearized Poisson-Boltzmann equation for a molecular system with different dielectric constants for the interior of the molecule ( $\epsilon_p$ ) and for the solvent ( $\epsilon_s$ ) by a finite difference method (Warwicker and Watson 1982). The model compounds for amino acids are the *N*-formyl *N*-methylamide derivatives of the respective amino acid in aqueous solution, whose  $pK_a$ -values can be determined experimentally.

*Monte-Carlo sampling.* The thermodynamic average in Eq. (1) can not be calculated exactly if the number of possible protonation states is too large. Even if there are only 20 titratable groups in a protein, an exact calculation is already very time consuming, since the number of possible protonation states is  $2^{20} \approx 10^6$ . Thus, we used a Metropolis Monte Carlo (MC) method, implemented in the program MCTI (Beroza et al. 1991), to calculate the protonation pattern. The statistical uncertainty of this method can be estimated by evaluating the protonation correlation function of each individual titratable group.

To improve sampling efficiency, the program MCTI allows one to change the protonation state of two strongly coupled titratable groups simultaneously in one MC move (Beroza et al. 1991). Such double MC moves are done in addition to simple MC moves. However, if small values are used for the dielectric constant of the protein as for instance  $\epsilon_p = 2$ , the coupling of titratable groups is so strong, that double moves alone are not sufficient to avoid sampling problems. Therefore, in addition to double moves, we introduced triple moves in the program MCTI, where three strongly coupled titratable groups change their protonation state simultaneously in one MC move. Three sites A, B, and C are defined as a strongly coupled triplet, if A and B as well as B and C are coupled stronger than a certain threshold energy. Note that strong coupling of A and C is not required to meet the criterion for a strongly coupled triplet. With these triple moves, sampling problems do not occur even with small  $\epsilon_p$ -values.

*Multiple conformations.* If multiple conformations of a protein are considered in the calculation of protonation patterns, Eq. (1) needs modifications. Besides the average over all protonation states  $q$ , also an average over conformations labeled by  $n$  must be performed Eq. (3).

$$\langle x_i \rangle = \frac{\sum_n \sum_q x_i \exp \left\{ -\beta \left[ \sum_{\mu} x_{\mu} \Delta G_{intr,\mu}(n) + \frac{1}{2} \sum_{v \neq \mu} q_{\mu} q_v W_{\mu v}(n) \right] + \Delta G_C(n) \right\}}{\sum_n \sum_q \exp \left\{ -\beta \left[ \sum_{\mu} x_{\mu} \Delta G_{intr,\mu}(n) + \frac{1}{2} \sum_{v \neq \mu} q_{\mu} q_v W_{\mu v}(n) \right] + \Delta G_C(n) \right\}} \quad (3)$$

Here,  $\Delta G_{intr,\mu}(n)$  is the energy needed to protonate group  $\mu$  at a given pH, while all other titratable groups are in their uncharged protonation state and the molecular system is in conformation  $n$ . The matrix element  $W_{\mu v}(n)$  is the electrostatic interaction between the groups  $\mu$  and  $v$  in conformation  $n$ . The conformational energy of the whole molecular system is accounted for by  $\Delta G_C(n)$  and

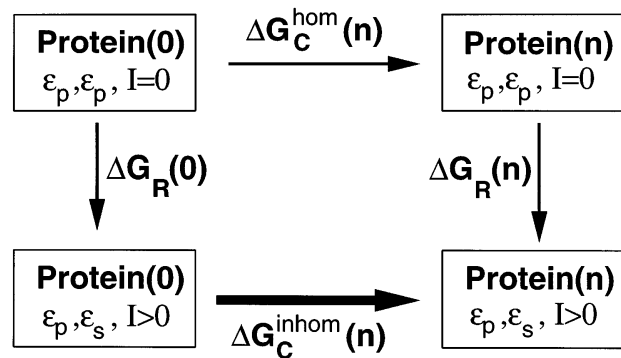


Fig. 1 Thermodynamic cycle to calculate the conformational energy

may also include non-electrostatic terms of the conformational energy (such as energy contributions from Lennard-Jones potentials or bond-length and bond-angle deformation). It is the relative conformational energy of the protonation reference state of conformation  $n$ , i. e., of the state, in which all titratable groups are in their uncharged protonation state. The energy of one conformation can be chosen arbitrarily. Hence,  $\Delta G_C(n)$  can be considered as the energy difference between the conformational energy of the conformation  $n$  itself and the energy of an arbitrarily chosen reference structure. This energy difference can be obtained via the thermodynamic cycle depicted in Fig. 1 resulting in Eq. (4). Artifacts from a discrete grid cancel by taking energy differences.

$$\Delta G_C^{inhom}(n) = G_C^{inhom}(n) - G_C^{inhom}(0) = \Delta G_C^{hom}(n) + \Delta G_R(n) - \Delta G_R(0) \quad (4)$$

According to Fig. 1, the protein with a dielectric constant  $\epsilon_p$  is brought from a medium with homogeneous dielectrics, where the ionic strength is  $I=0.0$  and the dielectric constant is  $\epsilon_p$  everywhere, into the solvent with a dielectric constant  $\epsilon_s$  and a ionic strength  $I \geq 0$ . In the homogeneous medium, the conformational energy difference  $\Delta G_C^{hom}(n)$  can be obtained analytically from a conventional force field like CHARMM (Brooks et al. 1983). To distinguish the conformational energy in a homogeneous medium from the required conformational energy in an inhomogeneous medium, these two energies are labelled as  $\Delta G_C^{hom}(n)$  and  $\Delta G_C^{inhom}(n)$ , respectively. The energy  $\Delta G_R$  (Eq. (5)) is required to bring a molecule from a medium with a dielectric constant  $\epsilon_p$  and ionic strength  $I=0.0$  into a medium with a dielectric constant of  $\epsilon_s$  and ionic strength  $I \geq 0$ .

$$\Delta G_R = \frac{1}{2} \sum_{i=1}^N q_i [\phi(\epsilon_p, \epsilon_s, I) - \phi(\epsilon_p, \epsilon_p, 0.0)] \quad (5)$$

In Eq. (5)  $\phi(\epsilon_p, \epsilon_s, I)$  is the solution of the Poisson-Boltzmann Equation with dielectric constants  $\epsilon_p$  for the protein and  $\epsilon_s$  for the solvent and ionic strength  $I$  using the charge distribution of the reference protonation-state. The sum in Eq. (5) runs over all charges of the molecular system in the reference protonation-state. The program MEAD, which we used to calculate intrinsic  $pK_a$ -values, is also able to calculate this energy. A thermodynamic cycle similar to

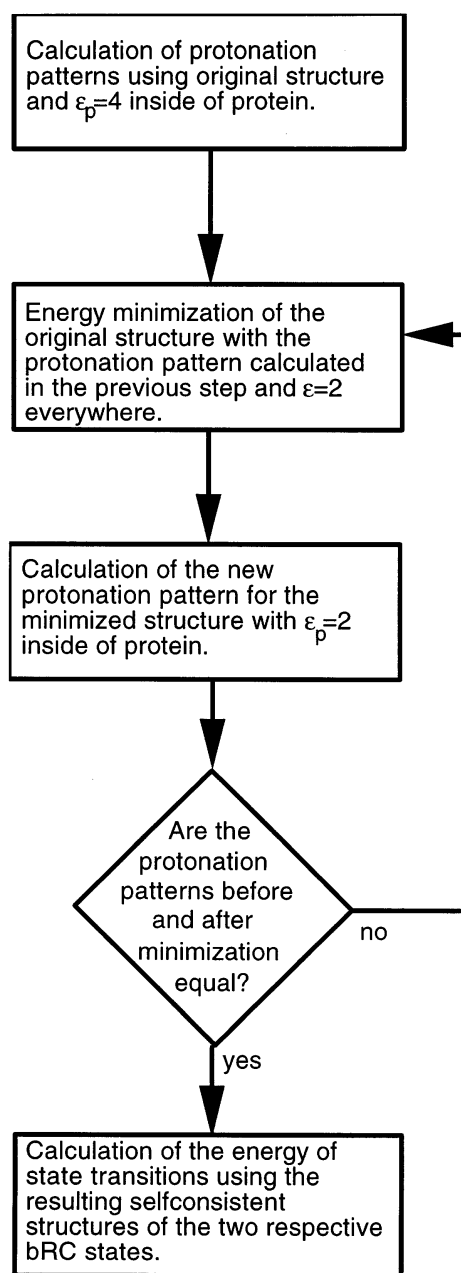


Fig. 2 Overview of the complete procedure

the one depicted in Fig. 1 has previously been used to calculate relative binding constants of diprotein complexes (Ullmann et al. 1997).

The above procedure differs from previous methods that include different conformations in the computation of protonation patterns (You and Bashford 1995; Beroza and Case 1996; Buono et al. 1994; Sham et al. 1997; Schaefer et al. 1997; Alexov and Gunner 1997). Here the conformations of different titratable groups can be correlated using, for instance, different molecular conformations from energy minimization or from a trajectory generated by molecular dynamics simulations or a Monte Carlo method. With the correlated conformations the enormous combin-

atorial increase of uncorrelated conformations of the individual titratable sites is avoided. But most important is that the present method can also account for the energetics of conformational changes of the non-titratable molecular groups, which generally can interact strongly with the titratable groups. Furthermore, a change of the inhomogeneous dielectrics going along with a change of the shape of the protein as well as contributions from non-electrostatic interactions (i. e., energy contributions from Lennard-Jones potentials and from bond-length and bond-angle deformation) can also be included in our treatment.

*Structural relaxation.* In the conventional method for calculating protonation patterns, structural relaxation upon changes in the electrostatic potential is not considered explicitly. Instead, it is incorporated only in an average way by using a dielectric constant of  $\epsilon_p \geq 4$ , which accounts for electronic as well as for nuclear polarization effects (Warshel and Russel 1984; Warshel et al. 1997). The latter are due to reorientation of charged and polar molecular groups. If only electronic polarizability is taken into account, the dielectric constant is  $\epsilon_p = 2$ , based on the high-frequency dielectric constant of apolar organic liquids (Sharp and Honig 1990).

In our method, nuclear polarization effects are treated explicitly by structural relaxation. This is achieved in the following manner. (i) To get reasonable starting values for the protonation pattern at a given pH-value a conventional calculation with  $\epsilon_p = 4$  is performed using the original unrelaxed crystal or NMR structure. (ii) Now the atomic partial charges of the titratable groups are assigned according to their fractional protonation. These atomic partial charges are obtained by a linearly weighted average of the charges of the protonated and deprotonated state. Starting with this charge assignment, we energetically minimized the structure using the program CHARMM (Brooks et al. 1983). To save CPU-time, we used homogeneous dielectrics for the energy minimization, which are valid only approximately. To avoid artifacts due to energy minimization, protein atoms close to the surface are spatially constrained. (iii) Next, the calculation of the protonation pattern is repeated with the minimized structure. However, the dielectric constant for the protein is now set to a value of  $\epsilon_p = 2$ , since the nuclear polarization is taken into account by the structural relaxation, which occurs during the minimization procedure. (iv) Steps (ii) and (iii) are repeated iteratively, until the calculated fractional protonation of each individual titratable group differs less than a tenth of a proton between subsequent iteration steps providing self-consistency of structure and protonation pattern. Figure 2 summarizes the algorithm.

Note that the energy minimization in step (ii) is performed with the protonation pattern calculated in the previous step, but with the original structure as starting conformation. In the absence of thermal fluctuations, protonation patterns and conformations are able to stabilize each other, so that rather artificial conformations become possible. Therefore, for each minimization the original unre-

laxed structure is used as starting conformation in order to prevent the structure from drifting into conformations that are too far away from the original structure.

### 3 Application

We applied our new methods to the bacterial photosynthetic reaction center (bRC). To obtain the driving force of the electron transfer reactions between the quinones, we calculated the protonation patterns of the bRC with the primary quinone ( $Q_A$ ) and the secondary quinone ( $Q_B$ ) in the different redox states ( $Q_A Q_B$ ,  $Q_A^- Q_B$ ,  $Q_A Q_B^-$ ,  $Q_A^- Q_B^-$ , and  $Q_A Q_B^{2-}$ ). Figure 2 provides a schematic overview of the total procedure.

**Structure.** In our calculations, we used the crystal structure of the bRC of *Rps. viridis* with a resolution of 2.3 Å (Deisenhofer et al. 1995), PDB entry 1prc. Since the cytochrome *c* subunit is more than 25 Å away from the quinone binding sites, we neglected this subunit in our calculations. All sulfate ions and detergent molecules were removed. For the electrostatic calculations, but not for energy minimization, all crystal water molecules were also removed. The influence of water and ions was considered in the electrostatic calculations by the continuum model. We used an extended atom representation for the non-polar hydrogen atoms except for quinones, chlorophylls, and pheophytins, where all hydrogens were treated explicitly. Coordinates of explicitly treated hydrogen atoms were generated with CHARMM (Brooks et al. 1983). The positions of the hydrogen atoms were subsequently energetically optimized with fixed positions of the heavy atoms.

In the crystal structure used, the  $Q_B$  binding pocket is occupied to only 30% (Deisenhofer et al. 1995). A structure with improved occupancy and resolution at the  $Q_B$  site has been solved but is not available yet (Lancaster et al. 1995; Lancaster and Michel 1996). Therefore, we adjusted the 1prc bRC structure at the  $Q_B$  site according to published data from Lancaster and Michel (1996) and Lancaster et al. (1995). We rotated  $Q_B$  around the axis through the methyl group at the quinone ring that is perpendicular to the ring plane, so that the methoxy group opposite to the methyl group was shifted 0.75 Å towards Ser L223. Furthermore the carboxyl group of Glu L212 was rotated by 90° around the bond between  $C_\gamma$  and  $G_\delta$ . This manipulated structure is called “original structure” to distinguish it clearly from the minimized structures occurring after application of the relaxation procedure.

**Atomic partial charges.** The atomic partial charges of the amino acids, including the protonated and deprotonated state of titratable amino acids, were adopted from the CHARMM 22 parameter set (MacKerell et al. 1992). The acidic hydrogen atom of protonated glutamate and aspartate was not represented explicitly. Instead, appropriate charges were assigned symmetrically at the two carboxyl oxygen atoms. The atomic partial charges that are not in-

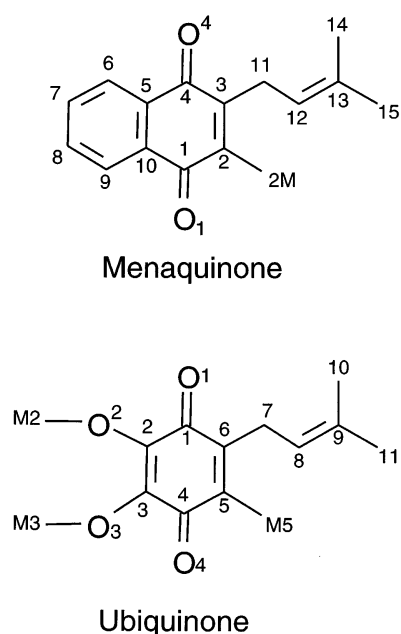


Fig. 3 Atom names used for MQ and UQ in Tables 1 and 2

cluded in the CHARMM 22 parameter set were calculated quantum-chemically with the program Spartan 4.0. We fitted the atomic partial charges to represent faithfully the electrostatic potential calculated from the wave functions using the CHELPG-like method (Breneman and Wiberg 1990) implemented in Spartan. The atomic partial charges of chlorophyll and pheophytin (Fig. 4) were calculated semiempirically at the PM3 level, those of the quinones (Fig. 3) in all considered redox states and of the deprotonated cysteine were calculated ab initio with the Hartree-Fock method using a 6-31G\*\* basis set. The atomic partial charges of the high spin non-heme iron (Kartha et al. 1991) and its ligands were calculated by a density functional method (LSDA/VWN) implemented in Spartan using the DN\*\* basis. The calculated partial charges of the iron center and the two quinones are listed in Tables 1 to 4. The neurosporen and the isoprene tails of MQ, chlorophyll and pheophytin were not considered in the quantum chemical calculations. The atomic partial charges of these apolar groups were set to zero.

**Calculations with fixed redox state of the quinones.** To yield the protonation patterns of the bRC in the states  $Q_A Q_B$ ,  $Q_A^- Q_B$ ,  $Q_A Q_B^-$ , and  $Q_A Q_B^{2-}$ , we fixed the quinones in their respective redox states and performed electrostatic calculations, MC sampling and structural relaxation. The MC sampling procedure and the relaxation by energy minimization were described above. Arginine, aspartate, cysteine, glutamate, histidine, lysine, tyrosine, and the C- and N-terminus, if not formylated, were considered as titratable groups. The histidines coordinating the magnesium ions of the chlorophylls and the glutamate and the histidines coordinating the non-heme iron were not considered as titratable. To determine the energetics of the electron transfer processes, the quinones were fixed in the unpro-



**Table 4** Atomic partial charges for bacteriochlorophyll-b and bacteriopheophytin-b, calculated by the semiempirical PM3 method. Atom names are adopted from PDB-standard given in Fig. 4. Hydrogen atoms are named according to their respective heavy atoms

Atom	Chloro- phyll	Pheno- phytin	Atom	Chloro- phyll	Pheno- phytin
Mg	0.10	–	C-MA	0.01	0.00
			3 H-MA	0.01	0.01
N-A	0.11	–0.49	C-MB	0.11	–0.02
C-HA	–0.22	0.11	3 H-MB	–0.01	0.03
C-1A	0.03	–0.02	C-MC	–0.05	–0.09
C-2A	0.10	0.14	3H-MC	0.02	0.03
H-2A	0.05	0.06	C-MD	–0.03	0.05
C-3A	–0.04	–0.22	3H-MD	0.03	0.01
H-3A	0.06	0.07			
C-4A	–0.10	0.56	C-AA	–0.13	0.06
			2 H-AA	0.09	0.02
N-B	0.12	–0.50	C-BA	–0.21	–0.30
H-B	–	0.36	2 H-BA	0.08	0.10
C-HB	–0.20	–0.65	C-GA	0.77	0.79
H-HB	0.19	0.21	O-1A	–0.53	–0.54
C-1B	–0.05	0.44	O-2A	–0.42	–0.43
C-2B	–0.16	–0.04	C-1	0.15	0.19
C-3B	–0.32	–0.39	2 H-1	0.01	0.01
C-4B	–0.02	0.40			
			C-AB	0.65	0.79
N-C	0.01	–0.35	C-BB	–0.14	–0.41
C-HC	–0.07	–0.46	3 H-BB	0.04	0.11
H-HC	0.20	0.17	O-BB	–0.57	–0.52
C-1C	–0.19	0.28			
C-2C	0.24	0.17	C-AC	–0.18	–0.11
H-2C	–0.01	0.02	H-AC	0.08	0.07
C-3C	–0.12	–0.22	C-BC	0.11	0.08
C-4C	0.05	0.17	3 H-BC	0.00	0.00
N-DB	0.01	0.52	C-AD	0.81	0.89
H-D	–	–0.01	O-BD	–0.52	–0.55
C-HD	–0.13	–0.20	C-BD	–0.73	–0.80
H-HD	0.18	0.20	H-BD	0.29	0.30
C-1D	–0.06	–0.25	C-GD	1.04	0.98
C-2D	0.18	0.05	O-1D	–0.57	–0.53
C-3D	–0.41	–0.43	O-2D	–0.50	–0.49
C-4D	0.21	–0.15	C-ED	0.19	0.27
			3 H-ED	0.00	–0.02

both centered on the titratable group. We used an ionic strength of 100 mM, an ion exclusion layer of 2 Å, and a solvent probe radius of 1.4 Å. The dielectric constant in the protein was set to  $\epsilon_p=4$  in the starting calculation and to  $\epsilon_p=2$  in the following calculations after energy minimization. The dielectric constant of the solvent was set to  $\epsilon_s=80$ . With the exception of the smaller value for the dielectric constant  $\epsilon_p$ , which accounts for the structural relaxation, these parameter values are similar to those used by Bashford and Karplus (1990) and also to those used in earlier calculations of the protonation pattern of the bRC (Beroza et al. 1995; Lancaster et al. 1996). We neglected the influence of the membrane, since calculations on the membrane protein bacteriorhodopsin with and without a membrane model yielded basically the same results (Bashford and Gerwert 1992; Sampogna and Honig 1994).

The MC sampling was done at pH 7.5. Pairs of titratable groups coupled stronger than 2.5 pK<sub>a</sub>-units were treated by double moves. The threshold for strongly cou-

pled triplets, treated by triple moves, was set to 5.0 pK<sub>a</sub>-units. In test calculations we found that these thresholds are suitable to get satisfactory convergence behaviour. One MC scan comprises as many random individual attempts for protonation changes (MC moves) as there are titratable groups considered. We did at first 5000 MC scans, considering all 194 titratable groups. Then we fixed the protonation of all groups whose average fractional protonation had a difference from unity or zero of less than 10<sup>–6</sup> in their respective protonation state. We excluded these groups from further MC sampling. With this reduced set of about 100 titratable groups, we performed another 50,000 MC scans. The reduced MC method is implemented in the program MCTI. The MC sampling was sufficient to reach a standard deviation of less than 0.01 protons at each individual titratable group. For most of the residues the standard deviation of a single group was much smaller than 0.01. The sum of the standard deviations for all fractional protonations was for each state of the bRC about 0.02 protons only.

For the energy minimizations, we used the program CHARMM (Brooks et al. 1983). Here, the dielectric constant was set to  $\epsilon=2$  everywhere. The Coulomb and Lennard-Jones interactions were calculated with a cut-off radius of 10.0 Å using group shift cut-off conditions. All atoms with a distance of more than 20 Å from the non-heme iron were constrained to their position of the original structure by a harmonic potential with a force constant of 0.42 kJ mol<sup>–1</sup> Å<sup>–2</sup>. We did not add water molecules to the system, but in contrast to the electrostatic calculations, the water molecules contained in the crystal structure were included in the energy minimization. These water molecules fill cavities in the protein and can thus account for an otherwise heterogeneous dielectric medium (Ullmann et al. 1996), which can not be handled with CHARMM. We performed 1000 steps of energy minimization with steepest descent, followed by 2000 steps with the conjugate gradient method.

*Redox potentials of the quinones in solution.* The continuum electrostatic method is able to yield reliable values merely for differences of reaction energies in different electrostatic environments. Therefore, we need the redox potentials of MQ and UQ in aqueous solution as reference values for computing the reaction energy of the electron transfer processes in the bRC. The redox potentials of quinones can not be measured in a protic solvent, since a reduced quinone has such a large pK<sub>a</sub>-value that it will inevitably take up a proton. The redox potentials in aprotic solvents, however, are known. These are –709 mV for MQ/MQ<sup>•–</sup> in DMF, –602 mV for UQ/UQ<sup>•–</sup> in DMF (Prince et al. 1983), and –1450 mV for UQ<sup>•–</sup>/UQ<sup>2•–</sup> in acetonitrile (Morrison et al. 1982). Therefore, we calculated the solvation energy of the quinones in the different redox states for water, acetonitrile and DMF as solvent by the continuum electrostatic method using the program MEAD. The dielectric constants used in these computations are  $\epsilon=80$  for water,  $\epsilon=38$  for acetonitrile, and  $\epsilon=37$  for DMF (CRC Handbook of Chemistry and Physics). The solvent radii are

1.4 Å for water, 2.0 Å for acetonitrile, and 2.8 Å for DMF. The calculated differences of the solvation energies are small, yielding the following redox potentials of the quinones corrected for water as solvent: -699 mV for MQ/MQ<sup>-</sup>, -592 mV for UQ/UQ<sup>-</sup>, and -1420 mV for UQ<sup>-</sup>/UQ<sup>2-</sup>.

**Energetics of electron transfer.** The calculation of protonation patterns yielded a different conformation for each bRC state. Thus, in order to calculate the energy of the electron transfer from Q<sub>A</sub> to Q<sub>B</sub>, we had to consider two different conformations according to Eq. (3). To obtain the value for the conformational energy difference  $\Delta G_C^{inhom}(n)$ , we calculated the energy difference  $\Delta G_R(n)$  using the program MEAD. We used initially a 200 Å cube grid with a 2.0 Å lattice spacing, followed by a 100 Å cube grid with a 0.5 Å lattice spacing. The centers of both grids were placed on the geometrical center of the bRC. For  $\Delta G_C^{hom}(n)$ , we used the full CHARMM energy (Brooks et al. 1983) with the same cut-off parameters as used for the energy minimization.

From the MC calculations with fixed quinone redox state, we could identify the titratable groups with a fractional protonation of less than 0.05 or more than 0.95 in all conformations and bRC states. These groups were supposed to contribute to the thermodynamic average in Eq. (3) only in their totally deprotonated or protonated state, respectively. Therefore, we fixed those titratable groups in the totally deprotonated or protonated state and did not consider them as titratable groups in subsequent calculations. Thus, only four titratable groups remained unfixed at pH 7.5. These residues are aspartate M182 and glutamates H97, M171, and M76. To prove the reliability of this approximation, we repeated the calculation of protonation patterns of all bRC states with this reduced set of unfixed titratable groups. The difference of the fractional protonation in this calculation compared to the MC calculation with the full set of titratable groups was less than 0.05 protons for each of the four unfixed residues.

In addition to the four unfixed titratable groups, the two quinones were included in the computation as a redox pair. In this case, the corresponding pH-dependent protonation energy  $\Delta G_{intr}$ , as defined in Eq. (2), is substituted by the pH-independent redox potential difference of the two quinones. The  $\Delta G_{intr}$  is calculated with the condition that the four titratable groups, which are varied in the calculation, are in their uncharged protonation state. The redox potential difference between the two quinones in the protein is obtained from their redox potential difference in aqueous solution by accounting for shift of the redox potential difference calculated from the continuum electrostatic method. In this case, the corresponding probability  $\langle x \rangle$  characterizes the equilibrium distribution of the redox states involved in the electron transfer process considered. The energy of electron transfer was obtained from  $\langle x \rangle$  by using Eq. (6).

$$\Delta G = -\frac{1}{\beta} \ln \frac{\langle x \rangle}{1 - \langle x \rangle} \quad (6)$$

Since the number of titratable group was small in this calculation, no MC sampling was necessary and the thermodynamic average (Eq. (3)) could be calculated exactly. The exact evaluation of Eq. (3) prevents sampling problems, which may occur with MC sampling if the energy of electron transfer is too large. If MC sampling were used, the energetically unfavored state is poorly sampled, and  $\langle x \rangle$  is close to unity or zero, leading to large uncertainties in the reaction energy calculated by Eq. (6) (Beroza et al. 1995).

## 4 Results and discussion

### Improved MC-sampling with triple moves

In Table 5, examples for residues with sampling problems are shown, when the calculations were performed with single moves only, with single and double moves, and with single, double and triple moves. For some residues, the sampling problems with single moves or single and double moves were so strong, that no statistical uncertainty could be calculated. For the calculation of the statistical uncertainty as described by Beroza et al. (1991), the correlation time is needed. The correlation time, however, can not be calculated, if the correlation function does not reach a lower limit (Beroza et al. 1991). As can be seen in Table 5, the introduction of double moves fixes some, but not all of the sampling problems. After introduction of triple moves, sampling problems did not occur any longer, and the statistical uncertainty was less than 0.01 for all residues.

### Relaxed selfconsistent structures

Consistency of energy minimized structure and protonation pattern was reached after eight iterations for each bRC state. We calculated root mean square (rms) deviations of the final structures corresponding to different bRC states relative to the original structure (i. e., the adapted crystal structure) and relative to each other (Table 6). To align two structures, we used the algorithm of Kabsch (1976). Water molecules were not considered in the calculation of rms deviations.

**Table 5** Examples of residues with MC sampling problems. Given are the protonation probabilities with statistical uncertainty ( $\pm 1\sigma$ ) for three residues with sampling problems in the first iteration of the Q<sub>A</sub><sup>-</sup>Q<sub>B</sub>-state, calculated from MC sampling with single, double and triple moves

Residue	Single	Double	Triple
Glu M171	(0.690) <sup>a</sup>	(0.726) <sup>a</sup>	0.649±0.005
δ-His H9	(0.660) <sup>a</sup>	0.742±0.005	0.741±0.005
δ-His M162	(0.314) <sup>a</sup>	(0.278) <sup>a</sup>	0.354±0.005

<sup>a</sup> Result is not converged, statistical uncertainty could not be calculated

**Table 6** Root mean square (rms) deviations (in Å) of the minimized structures respective to the crystal structure (column "x-ray") and to each other. Water molecules are not included in the calculation of the rms deviation

Structure	X-ray	Q <sub>A</sub> Q <sub>B</sub>	Q <sub>A</sub> <sup>-</sup> Q <sub>B</sub>	Q <sub>A</sub> Q <sub>B</sub> <sup>-</sup>	Q <sub>A</sub> <sup>-</sup> Q <sub>B</sub> <sup>-</sup>	Q <sub>A</sub> Q <sub>B</sub> <sup>2-</sup>
Q <sub>A</sub> Q <sub>B</sub>	0.670	0.000	0.096	0.096	0.154	0.122
Q <sub>A</sub> <sup>-</sup> Q <sub>B</sub>	0.668	0.096	0.000	0.132	0.174	0.147
Q <sub>A</sub> Q <sub>B</sub> <sup>-</sup>	0.665	0.096	0.132	0.000	0.132	0.109
Q <sub>A</sub> <sup>-</sup> Q <sub>B</sub> <sup>-</sup>	0.671	0.154	0.174	0.132	0.000	0.130
Q <sub>A</sub> Q <sub>B</sub> <sup>2-</sup>	0.676	0.122	0.147	0.109	0.130	0.000

The rms deviation of the final selfconsistent structures relative to the crystal structure, averaged over all atoms, is about 0.67 Å for all bRC states. However, the minimized structures are not equal for the different bRC states. The rms deviation among the minimized structures is up to 0.17 Å. Although Stowell et al. (1997) recently reported dramatic conformational changes upon the first electron transfer from Q<sub>A</sub> to Q<sub>B</sub>, the conformational changes calculated here are relatively small. This is not surprising, since minimization is only able to find the next minimum, but not to overcome energy barriers, which is necessary to obtain larger conformational changes. To consider larger conformational changes, molecular dynamics or MC dynamics may be useful.

#### Total protonation and individual site protonation

Table 7 shows the protonation probability of all non-standard protonated residues that are less than 25 Å away from the quinones. Furthermore, the difference in total protonation between the ground state Q<sub>A</sub>Q<sub>B</sub> of the bRC and the other states are listed. Significant differences in the proto-

nation pattern near the quinones between the original structure before relaxation (with  $\epsilon_p=4$ ) and the final selfconsistent structures after relaxation (with  $\epsilon_p=2$ ) occurred only at four residues (Glu H177, Glu H234, His L211, His M16). The histidine changed between  $\delta$ - and  $\epsilon$ -tautomer, but they remained nearly unprotonated. The two glutamates changed from an intermediate protonation probability in the original structure to a (nearly) complete protonation in the relaxed structure. Hence, our relaxation method tends to stabilize fully deprotonated or protonated states, as can also be seen in a less pronounced way for most of the other residues. Glu H177 and Glu H234 are responsible for most of the change in total protonation for the unrelaxed structure. Owing to the described stabilization effect, for the relaxed structures, both residues are almost fully protonated in all bRC states. Hence, the stabilization effect is responsible for the much smaller changes in total protonation of the bRC, if structural relaxation is applied (see last two rows of Table 7). At first glance, this effect seems surprising, since a decrease of electrostatic screening by reducing the dielectric constant of the protein from  $\epsilon_p=4$  to  $\epsilon_p=2$  will lead to increased differences in the protonation pattern due to changing the redox state of the quinones. The structural relaxation seems to replace the dielectric screening by using the larger dielectric constant of  $\epsilon_p=4$ . As a further consequence, changes in total protonation were reduced to values as small as the statistical uncertainty. However, the absence of proton uptake upon changing of the initial state Q<sub>A</sub>Q<sub>B</sub> is not in agreement with experimental results. At pH 7.5, Maróti and Wraight (1988) and McPherson et al. (1988) measured a total proton uptake of 0.34 for the transition from the Q<sub>A</sub>Q<sub>B</sub>-state to the Q<sub>A</sub><sup>-</sup>Q<sub>B</sub>-state of the bRC of *Rb. sphaeroides*. Sebban et al. (1995) measured this value for the bRC of *Rb. capsulatus* to be 0.24 protons. Using an unrelaxed bRC

**Table 7** Total protonation of the bRC and individual site protonations at pH 7.5 before relaxation by energy minimization ( $\epsilon_p=4$ ) and after relaxation ( $\epsilon_p=2$ ). All residues within a distance of 25 Å from one of the two quinones and with at least 0.05 protons deviation from standard protonation are shown, except N-termini of L- and M-chain which are completely deprotonated in all states before and after relaxation. For histidines, not the protonation, but the fraction of  $\delta$ -/ $\epsilon$ -tautomer is given. The remaining part (one minus fraction of  $\delta$ -tautomer minus fraction of  $\epsilon$ -tautomer) is the fraction of protonated histidine (i.e., with a proton at the  $\delta$ -N and at the  $\epsilon$ -N). Histidines protonated only at N<sub>ε2</sub> are considered to be in standard protonation and not included in the table

Residue	Relaxation	Q <sub>A</sub> Q <sub>B</sub>	Q <sub>A</sub> <sup>-</sup> Q <sub>B</sub>	Q <sub>A</sub> Q <sub>B</sub> <sup>-</sup>	Q <sub>A</sub> <sup>-</sup> Q <sub>B</sub> <sup>-</sup>	Q <sub>A</sub> Q <sub>B</sub> <sup>2-</sup>
Glu H45	before	0.05	0.06	0.05	0.06	0.05
	after	0.00	0.00	0.00	0.00	0.00
Glu H97	before	0.01	0.01	0.01	0.01	0.01
	after	0.03	0.04	0.06	0.04	0.03
Glu H177	before	0.03	0.06	0.59	0.80	0.99
	after	1.00	1.00	1.00	1.00	1.00
Glu H234	before	0.27	0.30	0.26	0.27	0.25
	after	0.98	0.98	0.98	0.99	0.98
Glu L104	before	1.00	1.00	1.00	1.00	1.00
	after	1.00	1.00	1.00	1.00	1.00
Glu L212	before	0.99	0.99	1.00	1.00	1.00
	after	1.00	1.00	1.00	1.00	1.00
His L211	before	0.47/0.53	0.50/0.50	0.53/0.47	0.53/0.47	0.58/0.42
	after	0.86/0.14	0.91/0.09	0.95/0.05	0.95/0.05	0.98/0.02
His M16	before	0.25/0.73	0.25/0.72	0.25/0.73	0.25/0.73	0.24/0.74
	after	0.13/0.87	0.13/0.87	0.14/0.86	0.15/0.85	0.14/0.86
all <sup>1</sup>	before	0.00	0.14	0.60	0.88	0.97
	after	0.00	0.02	0.05	0.02	0.03

<sup>1</sup> Expressed as difference to the ground state Q<sub>A</sub>Q<sub>B</sub>, statistical uncertainty ( $\pm 1\sigma$ ) is  $\pm 0.02$

structure, the calculated value of the total proton uptake agrees better with experimental results. The proton uptake for the transition from the  $Q_A Q_B$ -state to the  $Q_A Q_B^-$ -state was determined to be 0.37 by McPherson et al. (1988) and 0.90 by Maróti and Wraight (1988). Both values were measured with the bRC of *Rb. sphaeroides*. The proton uptake upon the first electron transfer from  $Q_A$  to  $Q_B$  ( $Q_A^- Q_B \rightarrow Q_A Q_B^-$ ) is therefore 0.03 (McPherson et al. 1988) or 0.56 (Maróti and Wraight 1988). From our calculations, we got a value of 0.46 protons with the unrelaxed structure and 0.03 with the relaxed structures. Hence, in this case the results from the relaxed structures agree with the measurements of McPherson et al. (1988), while the results from the unrelaxed structure agree with the measurements of Maróti and Wraight (1988). In addition to the problem that different experimental groups obtained different results, a comparison with these experimental data may be problematic owing to the differences between the bRC of *Rps. viridis* used in our calculations and the bRC's of the purple bacteria used in the experiments (*Rb. sphaeroides* or *Rb. capsulatus*). Also a partial protonation of the charged quinones may contribute to the experimental values, but was not considered in our study.

#### Energetics of the electron transfers

We considered the first and the second electron transfer from  $Q_A$  to the unprotonated  $Q_B$ . The first electron transfer is the transition from the  $Q_A^- Q_B$ -state to the  $Q_A Q_B^-$ -state. We calculated the driving force of the electron transfer with these two structures. The reference protonation and redox state of both structures, used in the electrostatic calculation and in the calculation of the relative conformational energy, is the state in which all titratable groups are in their uncharged protonation state and the quinones are in the redox state  $Q_A Q_B$ . The conformation obtained by minimizing the energy with the quinones in the  $Q_A Q_B^-$ -state is considered as conformation 0 according to Fig. 1. Then we obtained  $-16$  kJ/mol for  $\Delta G_C^{hom}(n)$ .  $\Delta G_R(0)$  is 20 kJ/mol lower than  $\Delta G_R(n)$ , so that  $G_C^{inhom}(n)$  is  $+4$  kJ/mol. We used this value in Eq. (3) to calculate the reaction energy of the first electron transfer, yielding  $-95$  mV (9.2 kJ/mol). If no structural relaxation was applied, i. e., using only the original structure with  $\epsilon_p = 4$ , we calculated an energy value of  $-160$  meV (Rabenstein et al. 1998). Experimentally a value of about  $-150$  meV was measured for the bRC of *Rps. viridis* (Baciou et al. 1991). The value from the calculation without structural relaxation is not necessarily better than the value obtained from the calculation with relaxation, since the deviation of both values from the experimental value are within experimental uncertainty. Baciou et al. (1991) measured the energy of the first electron transfer as approximately the same at pH 7.5 and pH 9. At pH 9, another group determined this energy to be about  $-120$  meV (Shopes and Wraight 1985), which is closer to the value calculated with structural relaxation. In analogy to the results for the protonation pattern, the calculation of the reaction energy of the first electron transfer yields sim-

ilar results with the relaxation procedure and a dielectric constant of  $\epsilon_p = 2$  for the protein as without relaxation and  $\epsilon_p = 4$ .

For the second electron transfer, the bRC structures of the states  $Q_A^- Q_B$  and  $Q_A Q_B^{2-}$  were considered. The reference protonation and redox state of both structures is the state where all titratable groups are in their uncharged protonation state and the quinones are in the redox state  $Q_A Q_B^{2-}$ . The conformation obtained by minimizing the energy with the quinones in the  $Q_A Q_B^{2-}$ -state is considered as conformation 0 according to Fig. 1. We obtained  $+206$  kJ/mol for  $\Delta G_C^{hom}(n)$ .  $\Delta G_R(0)$  is 13 kJ/mol higher than  $\Delta G_R(n)$ , so that  $G_C^{inhom}(n)$  is  $+193$  kJ/mol. Together with the electrostatic calculation, this resulted in a total reaction energy of  $+1.2$  eV (120 kJ/mol) for the second electron transfer from  $Q_A$  to the unprotonated  $Q_B$ . Without relaxation, we calculated an energy value of  $+1.1$  eV (110 kJ/mol). Again without structural relaxation and  $\epsilon_p = 4$ , the results are similar to the results with structural relaxation and  $\epsilon_p = 2$ . The results also supports our conclusion from a recent study without relaxation (Rabenstein et al. 1998), where we found that the reaction energy for the second electron transfer from  $Q_A$  to the unprotonated  $Q_B$  is too large to allow a double reduced, unprotonated  $Q_B$  as a thermally accessible intermediate. Hence, the second electron transfer will not occur before protonation of the single reduced  $Q_B$ . Even with explicit consideration of structural relaxation, our conclusions obtained from unrelaxed bRC structures remain unchanged.

## 5 Conclusion

In this study we formulated an expression to calculate protonation patterns of interacting titratable groups in a protein for an ensemble of different molecular conformations (Eq. (3)). We presented a method to obtain energetically minimized structures that are determined selfconsistently with their protonation pattern. The structural relaxation resulting from this procedure accounts for nuclear polarization effects. Thus, the dielectric constant in the protein could be reduced from a value of  $\epsilon_p = 4$ , typically used in the absence of structural relaxation, to a value of  $\epsilon_p = 2$  accounting only for electronic polarization effects with basically the same results. To overcome convergence problems occurring if the MC method for sampling the protonation states of a molecular system is used in conjunction with a dielectric constant as small as  $\epsilon = 2$ , we introduced triple moves involving a simultaneous change of the protonation state of three strongly coupled titratable groups.

We applied our method to the bRC of *Rps. viridis* to calculate protonation patterns for different redox states of the primary and secondary quinone  $Q_A$  and  $Q_B$ . The present application demonstrates that the results from a conventional calculation with a dielectric constant of  $\epsilon_p = 4$  for the protein without structural relaxation are similar to the results from a calculation with a dielectric constant of  $\epsilon_p = 2$  for the protein with structural relaxation. In more detail,

we observed that the effective dielectric screening is even slightly stronger for  $\epsilon_p=2$  with the procedure of self-consistent structural relaxation than for  $\epsilon_p=4$  without relaxation.

Generally, it is expected that the probability of a titratable group being in standard protonation is higher if a large dielectric constant for the protein is used. Although we used a low dielectric constant of  $\epsilon_p=2$  for the protein, the number of titratable groups that have a fractional protonation in the protein significantly (more than 0.1 protons) different from that in solution and are closer than 25 Å to one of the quinones is only six (Table 7). However, we have to keep in mind that with the present procedure to calculate protonation patterns the initial protonation pattern obtained with the higher dielectric constant  $\epsilon_p=4$  and the unrelaxed structure tends to be stabilized. A related effect could be observed by Wlodek et al. (1997).

Individual titratable groups that are partially protonated in the unrelaxed protein structure tend to be fully protonated or deprotonated in the self-consistently relaxed structure, leading to a structure and protonation pattern of lower energy. This may be a result of the structural relaxation method, where the protonation pattern and the structure are energetically minimized, corresponding effectively to a dynamic at vanishing temperature and therefore correlating structure and protonation pattern too strongly. With a molecular ensemble at non-vanishing temperature, these correlations are reduced due to suitable entropic contributions. Such an ensemble can not be generated easily with molecular dynamics solving Newton's equation of motion. During a molecular dynamics simulation, it is impossible to change the protonation pattern discontinuously. This problem does not occur with MC dynamics. An efficient off-lattice MC dynamics method for proteins was recently developed in our group (Knapp and Irgens-Defregger 1991; Hoffmann and Knapp 1996a, 1996b, 1997; Sartori et al. 1998), and we are now working on combining this MC dynamics with MC titration.

MC dynamics will also solve another problem which appears with structural relaxation by energy minimization. In contrast to energy minimization, molecular dynamics and MC dynamics are able to overcome energy barriers. This is often necessary, even if only apparently small conformational changes are involved. To demonstrate this, we also tried to calculate the energetics of protonation reactions of the  $Q_B$  in the bRC (results not shown). Our relaxation procedure was not able to give energetically favorable self-consistent structures for the protonated states of  $Q_B$ , so that the states where  $Q_B$  was unprotonated were favored strongly against those states where  $Q_B$  was protonated, resulting in an unrealistic high energy for the protonation of  $Q_B$ . A similar result was obtained by Cometta-Morini et al. (1993), who also applied a minimization scheme for structural relaxation and found that the singly reduced  $Q_B$  is completely deprotonated over the pH range from 6 to 11. However, in a recent study, we calculated the protonation energies for  $Q_B$  in the bRC without structural relaxation and got energy values that are consistent with experimental data (Rabenstein et al. 1998). Assuming that

for the protonation of  $Q_B$  a conformational energy barrier must be overcome, energy minimization is not sufficient to obtain properly relaxed structures. Therefore, a relaxation procedure needs to be applied that generates protein conformations at non-vanishing temperature.

**Acknowledgements** This work was supported by the Deutsche Forschungsgemeinschaft SFB 312, Project D7. G. M. U. is supported by a fellowship of Boehringer Ingelheim Fonds. We thank Donald Bashford, Paul Beroza and Martin Karplus for providing the programs MEAD, MCTI, and CHARMM, respectively. We are grateful to Ingo Muegge for useful discussions.

## References

- Alexov EG, Gunner MR (1997) Incorporating protein conformational flexibility into the calculation of pH-dependent protein properties. *Biophys J* 74: 2075–2093
- Antosiewicz J, Briggs JM, Elcock AH, Gilson MK, McCammon JA (1996) Computing ionization states of proteins with a detailed charge model. *J Comput Chem* 17: 1633–1644
- Antosiewicz J, McCammon JA, Gilson MK (1994) Prediction of pH-dependent properties of proteins. *J Mol Biol* 238: 415–436
- Baciou L, Sinning L, Sebban P (1991) Study of  $Q_B$  stabilization in herbicide-resistant mutants from the purple bacterium *Rhodospseudomonas viridis*. *Biochemistry* 30: 9110–9116
- Bashford D, Case DA, Dalvit C, Tennant L, Wright PE (1993) Electrostatic calculations of side-chain  $pK_a$  values in myoglobin and comparison with NMR data for histidines. *Biochemistry* 32: 8045–8056
- Bashford D, Gerwert K (1992) Electrostatic calculations of the  $pK_a$  values of ionizable groups in bacteriorhodopsin. *J Mol Biol* 224: 473–486
- Bashford D, Karplus M (1990)  $pK_a$ s of ionizable groups in proteins: atomic detail from a continuum electrostatic model. *Biochemistry* 29: 10219–10225
- Bashford D, Karplus M (1991) Multiple-site titration curves of proteins: an analysis of exact and approximate methods for their calculations. *J Phys Chem* 95: 9557–9561
- Beroza P, Fredkin DR, Okamura MY, Feher G (1991) Protonation of interacting residues in a protein by a Monte Carlo method: application to lysozyme and the photosynthetic reaction center. *Proc Natl Acad Sci USA* 88: 5804–5808
- Beroza P, Fredkin DR, Okamura MY, Feher G (1995) Electrostatic calculation of amino acid titration and electron transfer  $Q_A Q_B \rightarrow Q_A Q_B$  in the reaction center. *Biophys J* 68: 2233–2250
- Beroza P, Case DA (1996) Including side chain flexibility in continuum calculations of protein titration. *J Phys Chem* 100: 20156–20163
- Breneman CN, Wiberg KB (1990) Determining atom-centered monopoles from molecular electrostatic potentials. Need for high sampling density in formamide conformational analysis. *J Comput Chem* 11: 361–373
- Brooks BR, Bruccoleri RE, Olafson BD, States DJ, Swaminathan S, Karplus M (1983) CHARMM: a program for macromolecular energy, minimization, and dynamics calculation. *J Comput Chem* 4: 187–217
- Buono GSD, Figueirisco FE, Levy R (1994) Intrinsic  $pK_a$ s of ionizable residues in proteins: an explicit solvent calculation for lysozyme. *Proteins Struct Funct Genet* 20: 85–97
- Cometta-Morini C, Scharnagl C, Fischer SF (1993) Proton transfer to ubiquinone  $Q_B$  in the photosynthetic reaction center of *Rps. viridis*: the role of electrostatic interactions. *Int J Quantum Chem Quantum Biol Symp* 20: 89–106
- Deisenhofer J, Epp O, Sinning I, Michel H (1995) Crystallographic refinement at 2.3 Å resolution and refined model of the photosynthetic reaction centre from *Rhodospseudomonas viridis*. *J Mol Biol* 246: 429–457

- Demchuk E, Wade RC (1996) Improving the continuum dielectric approach to calculating  $pK_a$ s of ionizable groups in proteins. *J Phys Chem* 100: 17 373–17 387
- Hoffmann D, Knapp EW (1996a) Polypeptide folding with off-lattice Monte Carlo dynamics: the method. *Eur Biophys J* 24: 387–403
- Hoffmann D, Knapp EW (1996b) Protein dynamics with off-lattice Monte Carlo moves. *Phys Rev E* 53: 4221–4224
- Hoffmann D, Knapp EW (1997) Folding pathways of a helix-turn-helix model protein. *J Phys Chem B* 101: 6734–6740
- Honig B, Nicholls A (1995) Classical electrostatics in biology and chemistry. *Science* 268: 1144–1149
- Kabsch W (1976) A solution for the best rotation to relate two sets of vectors. *Acta Cryst A* 32: 922–923
- Kartha S, Das R, Norris JR (1991) Electron transfer in photosynthetic reaction centers. In: Sigel H (ed) *Metal ions in biological systems*, vol 27, chapter 10, pp 323–359
- Klapper I, Fine R, Sharp KA, Honig BH (1986) Focusing of electric fields in the active site of Cu-Zn superoxide dismutase: effects of ionic strength and amino-acid modification. *Proteins Struct Funct Genet* 1: 47–59
- Knapp E, Irgens-Defregger A (1991) Long time dynamics of proteins: an off-lattice Monte Carlo method. In: Harms U (ed) *Super-computer and chemistry*, vol 2. Springer, Berlin Heidelberg New York, pp 83–106
- Lancaster CRD, Ermler U, Michel H (1995) The structures of photosynthetic reaction centers from purple bacteria as revealed by X-ray crystallography. In: Blankenship RE, Madigan MT, Bauer CE (eds) *Anoxygenic photosynthetic bacteria*, chapter 23. Kluwer, Dordrecht, pp 503–526
- Lancaster CRD, Michel H (1996) New insights into the X-ray structure of the reaction center from *Rhodospseudomonas viridis*. In: Michel-Beyerle M-E (ed) *The reaction center of photosynthetic bacteria*. Springer, Berlin Heidelberg New York, pp 23–35
- Lancaster CRD, Michel H, Honig B, Gunner MR (1996) Calculated coupling of electron and proton transfer in the photosynthetic reaction center of *Rhodospseudomonas viridis*. *Biophys J* 70: 2469–2492
- Lide DR (1992) *CRC handbook of chemistry and physics*, 73rd edn. CRC Press, Boca Raton
- MacKerell AD, Bashford D, Bellott M, Dunbrack RL, Field MJ, Fischer S, Gao J, Guo H, Ha S, Joseph D, Kuchnir L, Kuczera K, Lau FTK, Mattos C, Michnik S, Ngo T, Nguyen DT, Prodhom B, Roux B, Schlenkrich M, Smith JC, Stote R, Straub J, Wiorkiewicz-Kuczera J, Karplus M (1992) Self-consistent parameterization of biomolecules for molecular modeling and condensed phase simulation. *FASEB J* 6: A143
- Maróti P, Wraight CA (1988) Flash-induced  $H^+$  binding by bacterial photosynthetic reaction centers: influences of the redox states of the acceptor-quinones and primary donor. *Biochim Biophys Acta* 934: 329–347
- McPherson PH, Okamura MY, Feher G (1988) Light-induced proton uptake by photosynthetic reaction centers from *Rhodobacter sphaeroides* R-26. I. Protonation of the one-electron states  $D^+Q_A^-$ ,  $DQ_A^-$ ,  $D^+Q_AQ_B^-$  and  $DQ_AQ_B^-$ . *Biochim Biophys Acta* 934: 348–368
- Morrison LE, Schelhorn JE, Cotton TM, Bering CL, Loach PA (1982) Electrochemical and spectral properties of ubiquinone and synthetic analogs: relevance to bacterial photosynthesis. In: Trumppower BL (ed) *Function of quinones in energy conserving systems*, chapter II. 2. Academic Press, New York, pp 35–58
- Muegge I, Apostolakis J, Ermler U, Fritsch G, Lubitz W, Knapp EW (1996) Shift of the special pair redox potential: electrostatic energy computations of the mutants of the reaction center of *Rhodobacter sphaeroides*. *Biochemistry* 35: 8359–8370
- Prince RC, Dutton PL, Bruce JM (1983) Menaquinones and plastoquinones in aprotic solvents. *FEBS Lett* 160: 273–276
- Rabenstein B, Ullmann GM, Knapp EW (1998) Energetics of electron transfer and protonation reactions of the quinones in the photosynthetic reaction center of *Rhodospseudomonas viridis*. *Biochemistry* 37: 2488–2495
- Sampogna RV, Honig B (1994) Environmental effects on the protonation states of active site residues in bacteriorhodopsin. *Biophys J* 66: 1341–1352
- Sartori F, Melchers B, Böttcher H, Knapp EW (1998) An energy function for dynamics simulations of polypeptides in torsion angle space. *J Chem Phys* (in press)
- Scarsi M, Apostolakis J, Caflisch A (1997) Continuum electrostatic energies of macromolecules in aqueous solution. *J Phys Chem A* 101: 8098–8106
- Schaefer M, Sommer M, Karplus M (1997) pH-Dependence of protein stability: absolute electrostatic free energy differences between conformations. *J Phys Chem B* 101: 1663–1683
- Sebban P, Maróti P, Hanson DK (1995) Electron and proton transfer to the quinones in the bacterial photosynthetic reaction centers: insight from combined approaches of molecular genetics and biophysics. *Biochimie* 77: 677–694
- Sham YY, Chu ZT, Warshel A (1997) Consistent calculation of  $pK_a$ 's of ionizable residues in proteins: semi-microscopic and microscopic approaches. *J Phys Chem B* 101: 4458–4472
- Sharp KA, Honig B (1990) Electrostatic interactions in macromolecules. *Ann Rev Biophys Biophys Chem* 19: 301–332
- Shopes RJ, Wraight CA (1985) The acceptor quinone complex of *Rhodospseudomonas viridis* reaction centers. *Biochim Biophys Acta* 806: 348–356
- Stowell MHB, McPhillips TM, Rees DC, Soltis SM, Abresch E, Feher E (1997) Light-induced structural changes in photosynthetic reaction center: implications for mechanism of electron-proton transfer. *Science* 276: 812–816
- Ullmann GM, Knapp EW, Kostić NM (1997) Computational simulation and analysis of the dynamic association between plastocyanin and cytochrome *f*. Consequences for the electron-transfer reaction. *J Am Chem Soc* 119: 42–52
- Ullmann GM, Muegge I, Knapp E-W (1996) Shifts of the special pair redox potential of mutants of rhodobacter sphaeroides calculated with Delphi and Charmm energy functions. In: Michel-Beyerle EM (ed) *The reaction centers of photosynthetic bacteria. Structure and Dynamics*. Springer, Berlin Heidelberg New York, pp 143–155
- Warshel A, Russell ST, Churg AK (1984) Macroscopic models for studies of electrostatic interactions in proteins: limitations and applicability. *Proc Natl Acad Sci USA* 81: 4785–4789
- Warshel A, Åqvist J (1991) Electrostatic energy and macromolecular function. *Annu Rev Biophys Biophys Chem* 20: 267–298
- Warshel A, Papazyan A, Muegge I (1997) Microscopic and semi-macroscopic redox calculations: what can and cannot be learned from continuum models. *JBIC* 2: 143–152
- Warshel A, Russell ST (1984) Calculations of electrostatic interaction in biological systems and in solution. *Q Rev Biophys* 17: 283–422
- Warwicker J, Watson HC (1982) Calculation of the electric potential in the active site cleft due to  $\alpha$ -helix dipoles. *J Mol Biol* 157: 671–679
- Wavefunction Inc, Irvine, CA (1995) Spartan version 4.0.
- Wlodek ST, Antosiewicz J, McCammon JA (1997) Prediction of titration properties of structures of a protein derived from molecular dynamics trajectory. *Protein Sci* 6: 373–382
- You T, Bashford DB (1995) Conformation and hydrogen ion titration of proteins: a continuum electrostatic model with conformational flexibility. *Biophys J* 69: 1721–1733